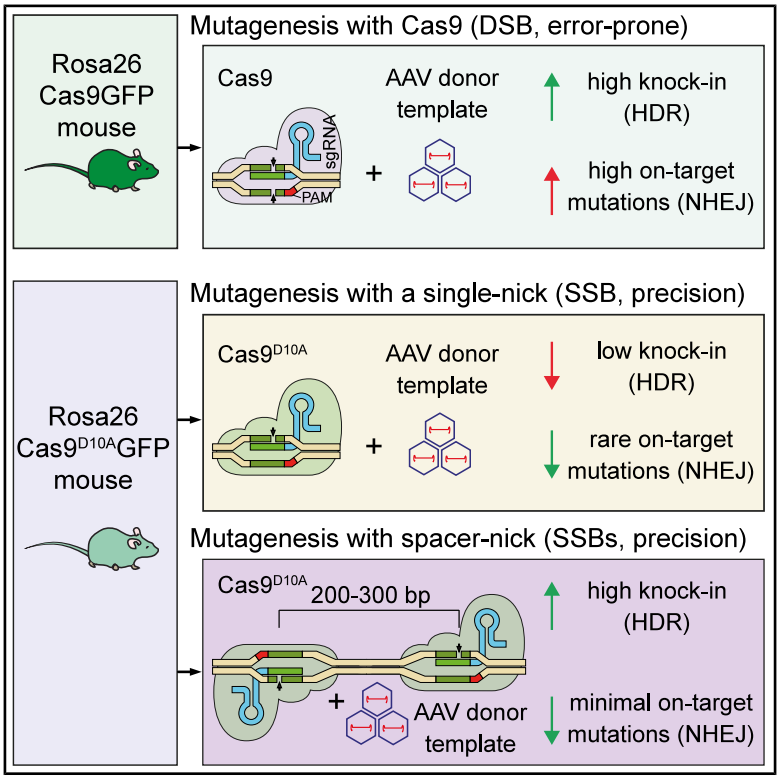
Cell Reports
Methods

Report

A Cas9^{D10A} nickase mouse line for precise genome editing

Graphical abstract



Highlights

- We generate a transgenic mouse line that ubiquitously expresses Cas9^{D10A} nickase
- Cas9^{D10A}-mediated gene knockin preserves efficient HDR in primary cells
- Cas9^{D10A}-mediated gene knockin reduces unwanted NHEJ events in primary cells

Authors

Janine Trombke, Daniel Bauersachs, Carlota Farre Diaz, Klaus Rajewsky, Van Trung Chu, Ralf Kühn

Correspondence

trombkj1@mskcc.org (J.T.), vantrung.chu@mdc-berlin.de (V.T.C.), ralf.kuehn@mdc-berlin.de (R.K.)

In brief

By combining single-nick and spacer-nick gene targeting approaches with AAV donor vectors in Cas9^{D10A} transgenic mouse cells, Trombke et al. preserve high-fidelity knockins with minimal unwanted mutational burden at on- and off-target sites in primary hematopoietic cells, establishing a versatile platform for disease modeling and therapeutic genome editing.

Trombke et al., 2027, Cell Reports Methods 7, 101668
January 25, 2027 © 2026 The Authors. Published by Elsevier Inc.
https://doi.org/10.1016/j.crmeth.2026.101668

CellPress

Please cite this article in press as: Trombke et al., A Cas9^{D10A} nickase mouse line for precise genome editing, Cell Reports Methods (2026), https://doi.org/10.1016/j.crmeth.2026.101668

Cell Reports Methods

CellPress
OPEN ACCESS

Report

A Cas9^{D10A} nickase mouse line for precise genome editing

Janine Trombke,[1,*] Daniel Bauersachs,[2] Carlota Farre Diaz,[1,3] Klaus Rajewsky,[1] Van Trung Chu,[1,2,*] and Ralf Kühn[2,4,*]
[1]Max-Delbrück Center for Molecular Medicine in the Helmholtz Association (MDC), Immune Regulation and Cancer, Berlin, Germany
[2]Max-Delbrück Center for Molecular Medicine in the Helmholtz Association (MDC), Genome Engineering and Disease Models, Berlin, Germany
[3]Max-Delbrück Center for Molecular Medicine in the Helmholtz Association (MDC), Biology of Malignant Lymphomas, Berlin, Germany
[4]Lead contact
*Correspondence: trombkj1@mskcc.org (J.T.), vantrung.chu@mdc-berlin.de (V.T.C.), ralf.kuehn@mdc-berlin.de (R.K.)
https://doi.org/10.1016/j.crmeth.2026.101668

MOTIVATION The CRISPR-Cas9 editing approach relies on double-strand breaks that are frequently repaired via error-prone non-homologous end joining (NHEJ), resulting in unintended mutations at both on- and off-target sites. This mutational burden limits the precision required to model disease-causing mutations in primary cells, and existing constitutive Cas9 mouse lines share the same limitation. We therefore generate a transgenic mouse line ubiquitously expressing Cas9^{D10A} nickase, which induces single-strand breaks that preferentially trigger high-fidelity DNA repair mechanisms. By combining this nickase mouse line with single-nick or spacer-nick gene targeting approaches and adeno-associated virus (AAV) donor template delivery, we achieve high-precision knockins in primary T cells, B cells, and hematopoietic stem and progenitor cells (HSPCs) while significantly reducing unwanted NHEJ products.

SUMMARY

CRISPR-Cas9-mediated gene editing involves DNA double-strand breaks (DSBs) whose repair can generate unintended on- and off-target mutations. Here, we report a transgenic mouse line ubiquitously expressing Cas9^{D10A} nickase, which creates targeted single-strand breaks (SSBs) to stimulate precise gene editing while substantially reducing the undesired editing products associated with Cas9 nuclease. We demonstrate the versatility of this resource in primary T cells, B cells, and hematopoietic stem and progenitor cells (HSPCs), achieving efficient (5%–50%) high-fidelity reporter integration and introduction of cancer-relevant mutations at the *Cd79b* and *Notch1* loci. By enabling precise, low-mutation-burden gene editing directly in primary cells, the Cas9^{D10A} nickase mouse line provides a resource for inserting mutations relevant for hematopoietic disorders and malignancies and may be utilized more broadly for precision genome engineering across primary cell types.

INTRODUCTION

CRISPR-Cas9 nucleases generate double-strand breaks (DSBs) at targeted genomic sites, which are repaired either by non-homologous end joining (NHEJ) or homology-directed repair (HDR).[1–4] NHEJ is error-prone and often produces micro-insertions or deletions (indels), leading to unintended on-target repair products. In addition, cleavage at off-target sites further limits the precision and safety of Cas9-mediated editing.[5–8] In the presence of a DNA donor template, DSBs can be precisely repaired by the HDR pathway, instead of NHEJ, but pathway choice is strongly influenced by the structure of the DNA ends and cell cycle phase.[9,10] Thus, despite its great impact, Cas9-mediated gene editing is constrained by the introduction of undesired mutations at on- and off-target sites. Although improved guide RNA design and high-fidelity Cas9 variants reduce some of these issues,[11–14] error-prone gene editing outcomes remain. Cas9 nickase mutants, generated by inactivating one of Cas9's nuclease domains (D10A or H840A), introduce targeted single-strand breaks (SSBs), rather than DSBs.[1,3,15] SSBs are predominantly repaired by high-fidelity pathways such as HDR, making nickases an attractive tool for precise knock-in approaches.[16,17] However, SSB-mediated gene editing ("single-nick") yields low HDR efficiency in mammalian cells.[18,19] Dual-nicking with paired single-guide RNAs (sgRNAs) at distances of 38–68 base pairs (bp) favors HDR, but the juxtaposed breaks are often converted into DSBs, reintroducing mutagenic repair events.[20,21] Constitutive Cas9-expressing mouse lines have

This is an open access article under the CC BY license (http://creativecommons.org/licenses/by/4.0/).
Open access funding enabled and organized by Projekt DEAL.

Please cite this article in press as: Trombke et al., A Cas9^{D10A} nickase mouse line for precise genome editing, Cell Reports Methods (2026), https://doi.org/10.1016/j.crmeth.2026.101668

substantially simplified genome editing in primary cells and *in vivo*.[22,23] Doxycycline-inducible sgRNA/Cas9 and sgRNA/Cas9^{D10A}-expressing mouse lines have been generated from modified embryonic stem cells to modulate the frequency and size of indels generated at target loci *in vivo* and to avoid off-target effects in loss-of-function studies.[24] However, this study didn't explore HDR-mediated sequence replacement for precise genome editing in primary cells, nor were different approaches using nickase-mediated HDR for sequence replacements systematically validated in primary immune cells.

To overcome these limitations, we previously established the "spacer-nick" approach that combines Cas9^{D10A} nickase with two sgRNAs spaced at larger distances of 200–350 bp in human immune cells.[25] When paired with single-stranded adeno-associated virus serotype 6 (AAV6) donor templates, spacer-nick achieves efficient HDR in human hematopoietic stem and progenitor cells (HSPCs) and T cells, while markedly reducing NHEJ-induced indels, vector integrations, and off-target mutations. Here, we extend this approach by generating a Cas9^{D10A} nickase mouse line through targeted modification of our *Rosa26-Cas9iresEGFP* allele[22] in zygotes. Cas9^{D10A} mice exhibit normal hematopoietic development and robust nickase expression across immune lineages and across different organs. Using single-nick and the previously established spacer-nick strategies, we achieved efficient knockins (5%–50%) at multiple loci in T cells, B cells, and HSPCs, with substantially reduced unwanted on-target mutagenesis. HDR/NHEJ ratios were highest in single-nick-treated T and B cells, whereas HSPCs showed the greatest improvement using spacer-nick gene targeting as compared with Cas9. Thus, Cas9^{D10A} nickase mice enable efficient and precise knockins in hematopoietic cells, overcoming barriers to accurate modeling of blood disorders.

RESULTS

Generation of the Cas9^{D10A} nickase mouse line

We generated the Cas9^{D10A} nickase mouse strain (Figure 1A) by introducing the D10A codon replacement in zygotes of our *Rosa26-Cas9iresEGFP* mouse strain,[22] using CRISPR-Cas9-mediated editing.[26,27] Zygotes were electroporated with sgRNAs targeting the Cas9^{WT} allele together with a single-stranded oligodeoxynucleotide (ssODN) donor carrying the D10A substitution (Figures S1A–S1C). The resulting Cas9^{D10A} allele is ubiquitously expressed from the *Rosa26* locus under control of the CAG promoter and is linked to an EGFP reporter (Figure 1A), which is removable by FLP recombinase. We obtained seven pups carrying a Cas9^{D10A} allele (Figures S1D and S1E) and used validated founders (#S6685 male and #S6597 female) for further matings with C57BL/6 mice to establish the Cas9^{D10A} transgenic line for subsequent experiments.

The Cas9^{D10A} mouse strain shows normal hematopoiesis

We confirmed that Cas9^{D10A} mice are healthy and show normal hematopoiesis. Cas9^{D10A} mice observed up to 90 weeks of age exhibited normal development, fertility, and litter sizes, with no detectable abnormalities. Flow cytometry was used to detect Cas9^{D10A} transgene expression through assessment of EGFP reporter positivity across all hematopoietic lineages in bone marrow and spleen (Figures 1B and S2). In addition, Cas9^{D10A} protein was ubiquitously expressed in various hematopoietic lineages (Figure 1C) and in tissues, including the liver, lung, kidney, and brain (Figure 1D). Flow cytometry-based hematopoietic lineage profiling showed that all major hematopoietic progenitor, lymphoid, and myeloid cells in spleen, bone marrow, lymph nodes, and thymus of Cas9^{D10A} mice were overall comparable to C57BL/6 controls (Figures S2A–S2F; Table S1), with minor deviations. Together, these findings demonstrate that Cas9^{D10A} mice display normal physiology and hematopoietic development.

Cas9^{D10A} nickase-mediated reporter gene knockin at the *Lamin B1* locus

To validate Cas9^{D10A} nickase activity in primary immune cells, we targeted the *Lamin B1* (*Lmnb1*) locus with a T2A-mCherry reporter construct (Figure 2A), as previously described.[28,29] To establish Cas9^{D10A} nickase-mediated spacer-nick gene editing[25] in mouse cells, we used an sgRNA pair targeting the *Lmnb1* at a distance of 231 bp (sg1 and sg2, Figure 2B). Both sgRNAs showed efficient gene editing of >60% in Cas9^{WT} transgenic LSK cells, as quantified by inference of CRISPR edit (ICE) scores and T7 endonuclease I (T7EI) analysis (Figure S3A). Targeting the *Lmnb1* locus with the T2A-mCherry reporter donor vector in Cas9^{WT} HSPCs led to 49% HDR events, while Cas9^{D10A} nickase-mediated single-nick and spacer-nick editing approaches yielded 6% and 38%, respectively (Figures 2C and 2D). In Cas9^{WT} T cells, 51% HDR events were measured in the *Lmnb1* locus, while 17% and 54% HDR events were detected in Cas9^{D10A} T cells, using the single-nick and spacer-nick gene targeting approaches, respectively. In B cells, HDR efficiencies were 22% with Cas9^{WT}, 6% with single-nick, and 24% with spacer-nick. Remarkably, single-nick editing in primary T cells, B cells, and LSK cells yielded HDR events in more than 5% of treated cells. HDR rates were confirmed by integration-specific PCR (Figures S3B–S3D), and correct insertion of the T2A-mCherry reporter construct was confirmed by sequencing of PCR products (Figure S3E).

Analysis of the on-target mutation rate was performed by next-generation sequencing (NGS)-based amplicon deep sequencing of the target site in the *Lmnb1* locus (Figure 2D) and revealed that Cas9^{WT} gene editing resulted in high levels of unwanted NHEJ events (42% in HSPCs, 76% in B cells, and 43% in T cells). Using Cas9^{D10A} and spacer-nick editing, the levels of undesired NHEJ repair products in HSPCs, B cells, and T cells were reduced by 3- to 5-fold and reached background levels upon single-nick-induced gene targeting. The HDR/NHEJ ratios showed that spacer-nick gene targeting was most effective in HSPCs, while single-nick was superior in T and B cells (Figure 2E). Together, these data demonstrate that Cas9^{D10A} nickase approaches can be used for improved HDR-mediated sequence insertion with reduced undesired NHEJ-derived products.

Insertion of *CD79B*-Y195H and *Notch1*-P2514*fs4 cancer-associated mutations into Cas9^{D10A} HSPCs

Somatic mutations in self-renewing HSPCs can initiate blood disorders and malignancies. To evaluate the potential of

Please cite this article in press as: Trombke et al., A Cas9^{D10A} nickase mouse line for precise genome editing, Cell Reports Methods (2026), https://doi.org/10.1016/j.crmeth.2026.101668

CellPress
OPEN ACCESS

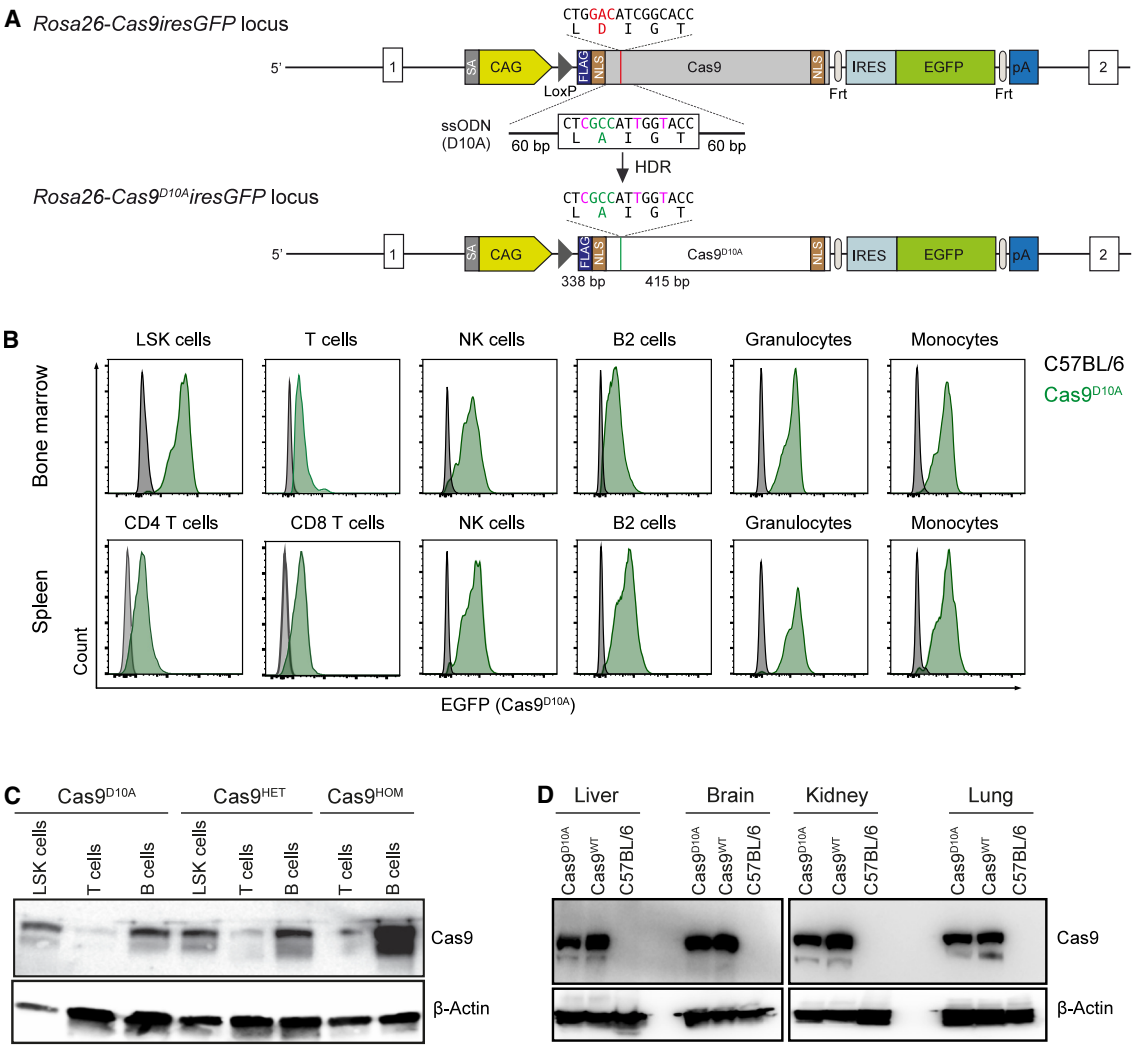


Figure 1. Generation of the Cas9^{D10A} transgenic mouse line

(A) Gene editing strategy replacing aspartic acid (D) codon (red) at position 10 with an alanine codon (green) through CRISPR-Cas9-mediated knockin in R26-Cas9iEGFP/C57BL/6 mouse zygotes.

(B) Representative flow cytometric analysis showing EGFP expression (Cas9^{D10A}) in cells isolated from bone marrow and spleen of transgenic Cas9^{D10A} mice (n = 6) in comparison to C57BL/6 (n = 6).

(C) Western blots showing Cas9 expression levels in LSK cells, T cells, and B cells isolated from heterozygous (HET) and homozygous (HOM) Cas9^{WT} and Cas9^{D10A} transgenic mice.

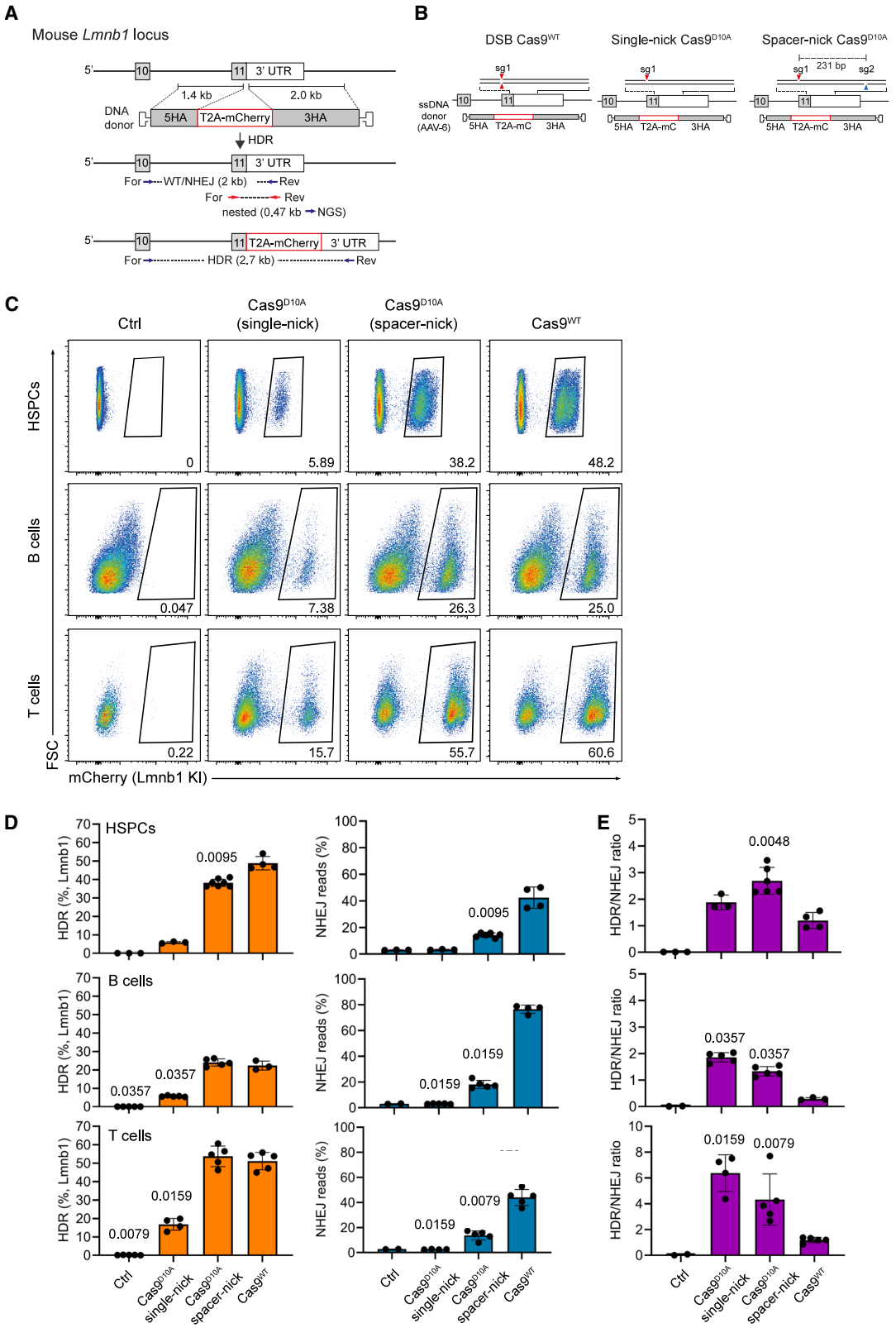
(D) Western blots showing Cas9 expression levels in the liver, brain, kidney, and lung tissues isolated from C57BL/6 (C57BL/6, negative control), Cas9^{WT}, and Cas9^{D10A} transgenic mice. β-Actin served as a loading control.

See also Figures S1 and S2.

Cas9^{D10A} nickase-mediated gene editing for modeling such mutations, we tested single-nick and spacer-nick targeting for the precise insertion of two recurrent cancer mutations—*CD79B*-Y195H in diffuse large B cell lymphoma (DLBCL)[30–32] and *NOTCH1*-P2514*fs4 in B cell chronic lymphocytic leukemia (B-CLL)[33–35]—into mouse HSPCs (Figures 3A and 3B). These genomic positions mutated in human DLBCL and B-CLL are conserved in the mouse *Cd79b* and *Notch1* genes (Figures 3A and 3B).

Pairs of sgRNAs flanking each mutational site were validated for high editing activity (>60%) using T7EI and ICE assays (Figures S4A, S4B, S5A, and S5B). To introduce these gene mutations, we stimulated HDR by the introduction of AAV donor templates carrying either the *Cd79b*-Y195H substitution with a diagnostic *BssSI* restriction site or the *Notch1*-P2514*fs4 mutation with a *BamHI* restriction site (Figures 3C and 3D). Screening for optimal sgRNA pairs in Cas9^{D10A} LSK cells identified combinations that supported efficient HDR-mediated Y195H insertion, with single-nick reaching up to 9% and spacer-nick up to 67% HDR (Figures S4C and S4D). Given the high endogenous expression of *Notch1* in T cells, sgRNA screening for the P2514*fs4 mutation insertion efficiency was initially performed in Cas9^{D10A}

Please cite this article in press as: Trombke et al., A Cas9^{D10A} nickase mouse line for precise genome editing, Cell Reports Methods (2026), https://doi.org/10.1016/j.crmeth.2026.101668



(legend on next page)

Please cite this article in press as: Trombke et al., A Cas9^{D10A} nickase mouse line for precise genome editing, Cell Reports Methods (2026), https://doi.org/10.1016/j.crmeth.2026.101668

CellPress
OPEN ACCESS

T cells, using an AAV-6 P2514*fs4-mCherry reporter DNA donor construct (Figure S5D). A second screen was then performed in Cas9^{D10A} LSK cells with an AAV-6 reporter-free P2514*fs4 DNA donor construct (Figure S5E), and the most efficient sgRNA pairs were selected for subsequent experiments in Cas9^{D10A} HSPCs to compare single-nick, spacer-nick, and Cas9-mediated gene targeting approaches (Figures 3C–3F).

Amplicon sequencing revealed ~10% HDR-mediated Y195H mutation insertion at the *Cd79b* locus in Cas9^{D10A}-expressing HSPCs with single-nick and >50% with a 197-bp sgRNA spacing and >40% with a 277-bp sgRNA spacing with spacer-nick, the latter being comparable to the HDR frequency rate observed in Cas9^{WT} HSPCs (>40%, Figure 3G). At the *Notch1* locus, single-nick produced ~4% HDR, and spacer-nick achieved 22% (167-bp spacing) or 19% (261-bp spacing), which was also comparable to the efficiency observed in Cas9^{WT} HSPCs (~19.5%, Figure 3H). The comparison of undesired NHEJ repair products (indels) confirmed, at both loci, marked differences between Cas9^{D10A} and Cas9^{WT} approaches (Figures 3G and 3H). Single-nick editing reduced on-target NHEJ products to near-background levels (<1%). Spacer-nick targeting also strongly decreased indel product frequencies compared with Cas9^{WT}, from 40% to <5% (197-bp sgRNA spacing) and 4.3% (277-bp spacing) at *Cd79b* (9- and 11-fold reductions) and from 69% to 12.6% (167-bp spacing) and 8.5% (261-bp spacing) at *Notch1* (5- and 8-fold reductions). Consequently, HDR/NHEJ ratios were markedly higher in both single-nick and spacer-nick conditions relative to Cas9 (Figures 3I and 3J), mirroring the data obtained at the *Lmnb1* locus. To evaluate overall editing fidelity, we further analyzed off-target mutation frequencies predicted *in silico* (Table S2) by NGS-based amplicon deep sequencing. Across several candidate loci, low off-target mutation rates were detected in Cas9^{WT}- or Cas9^{D10A}-expressing cells, and these were comparable to control frequencies, except for OT-3 predicted by targeting the *Notch1* locus with the common sgRNA1 (Figure S6). We detected about 5% off-target mutations in *Notch1*-targeted Cas9^{WT} cells, whereas a mutation rate comparable to background (1%) was detected in Cas9^{D10A}-expressing cells.

Together, these findings demonstrate that the Cas9^{D10A} nickase mouse line provides a platform for efficient and precise introduction of oncogenic point mutations into HSPCs, with minimized NHEJ-mediated on-target modification, for improved generation of model systems to study hematologic malignancies.

DISCUSSION

Genetic modification using CRISPR-Cas9 technology in zygotes has become state of the art for generating transgenic animals due to its speed and cost effectiveness.[22,26,36–39] We previously reported the *Rosa26-Cas9iresEGFP* transgenic mouse, generated by HDR-mediated integration of Cas9 into the *Rosa26* locus of C57BL/6 zygotes.[22] Here, we introduced the D10A mutation into the *Rosa26-Cas9iresEGFP* allele to generate a Cas9^{D10A} nickase-expressing mouse line. The resulting Cas9^{D10A} nickase transgenic mice were viable and fertile and displayed normal hematopoiesis. Because the transgene is expressed from the *Rosa26* locus under the control of the ubiquitous CAG promoter, the model provides broad Cas9^{D10A} nickase activity across tissues. While this study focused on primary hematopoietic lineages, the Cas9^{D10A} nickase-mediated targeting could also be further applied to other tissues in future studies.

Despite CRISPR-Cas9 technology revolutionizing genome editing, the reliance on DSBs introduces unintended sequence modifications and chromosomal translocations that limit its precision and translational potential. Powerful base- or prime-editing strategies are currently under development.[40–42] However, these systems are constrained by target-sequence restrictions and are not suited for donor template-dependent integrations that stimulate HDR. Our findings demonstrate that Cas9^{D10A}-mediated single- and spacer-nick gene editing approaches enable robust sequence insertions of reporter genes and cancer-relevant mutations in hematopoietic lineages, with low frequencies of undesired on-target indels. Both strategies promote high HDR/NHEJ ratios, yet they exhibit distinct lineage-specific strengths: the spacer-nick configuration leads to high HDR efficiency comparable to Cas9^{WT} in HSPCs, whereas the single-nick approach achieves exceptional fidelity in T and B cells and is also nearly error-free in HSPCs. These complementary features provide a framework for optimizing genome editing outcomes according to cell type and experimental goal. By inducing SSBs rather than DSBs, Cas9^{D10A} nickase achieves a favorable balance between efficiency and precision, enabling the introduction of single-nucleotide substitutions, reporter cassettes, or disease mutations without off-target effects caused by DSB repair, such as translocations and large deletions. Importantly, this system enables the precise modeling of oncogenic mutations directly in primary HSPCs. Using HDR-mediated DNA donor template integration, we introduced precise *Cd79b*-Y195H and *Notch1*-P2514*fs4 mutations, two recurrent driver mutations in

Figure 2. Cas9^{D10A} nickase enables efficient and precise reporter integration at the *Lmnb1* locus in hematopoietic cells

(A) Schematic of the editing strategy of the mouse *Lmnb1* locus. The locations of sgRNA target sites (black arrows), the rAAV donor homology arms, and the PCR strategy to validate genome editing outcomes are indicated.

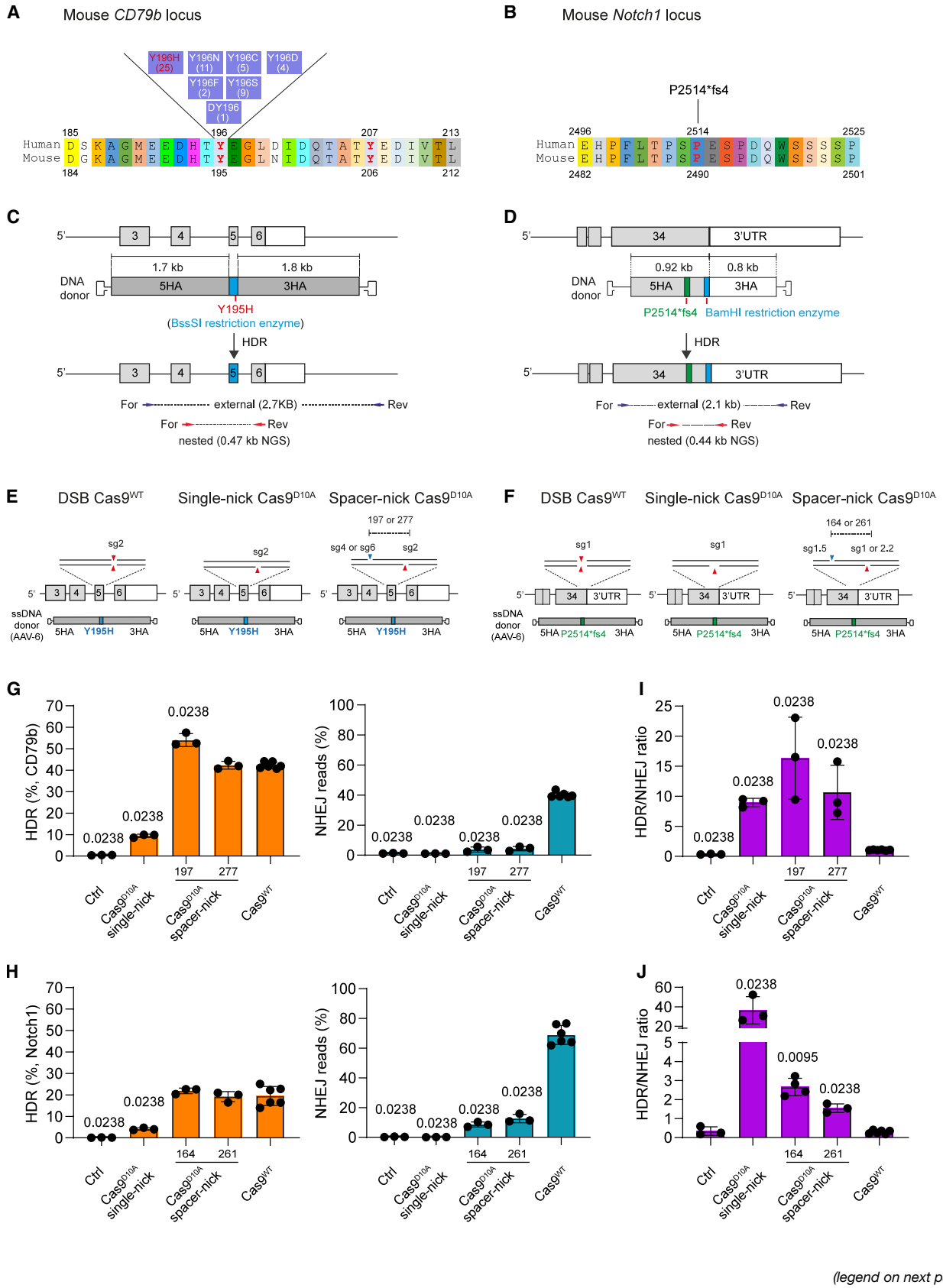
(B) Schematics presenting the *Lmnb1* gene editing approaches: double-strand break (DSB) in Cas9^{WT}-transgenic cells (left), and single-strand break (SSB) in Cas9^{D10A} nickase-transgenic cells for single-nick (middle) and spacer-nick (right).

(C and D) Assessment of mCherry-(*Lmnb1* knockin)-expressing HSPCs, T cells, and B cells through flow cytometry, and (D) quantification (left); NHEJ events were quantified through amplicon NGS analysis (right).

(E) HDR/NHEJ ratios of the three gene editing approaches. Data were pooled from 2–3 independent experiments and are represented as mean ± SD. Each symbol represents one mouse. Statistical analyses compared each group to Cas9^{WT}, using a two-tailed Mann-Whitney *U* test. *p* values are shown for comparisons reaching $p < 0.05$; all other comparisons were performed but did not reach statistical significance (see also Table S1).

See also Figure S3.

Please cite this article in press as: Trombke et al., A Cas9^{D10A} nickase mouse line for precise genome editing, Cell Reports Methods (2026), https://doi.org/10.1016/j.crmeth.2026.101668



(legend on next page)

Please cite this article in press as: Trombke et al., A Cas9^{D10A} nickase mouse line for precise genome editing, Cell Reports Methods (2026), https://doi.org/10.1016/j.crmeth.2026.101668

B cell malignancies, with efficiencies of up to 50%, while reducing NHEJ-induced on-target modification to a minimum. These results establish Cas9^{D10A} nickase-mediated targeting as a reliable experimental approach for the introduction of pathogenic mutations to study their impact on hematopoietic differentiation, clonal competition, and malignant transformation. Several groups have demonstrated success in Cas9-based *in vivo* HDR-mediated sequence replacements in somatic cells.[43–45] We have not performed somatic editing *in vivo* in the present study, and nickase-mediated HDR in the tissues of an adult animal has not been reported. The allele described here is intended to make such experiments tractable because Cas9^{D10A} is supplied from the endogenous locus, and the viral cargo remains available for guide RNAs and donor template. This removes principal constraints on delivering gene editing components of a nicking-based editing system to somatic tissues.

Overall, our Cas9^{D10A} nickase mouse line provides an experimental resource for high-fidelity genome editing in primary cells. It combines the precision of single-strand nicking with the flexibility of HDR-based DNA donor template integration, enabling safe and efficient genome editing. In addition to *in vitro* applications, Cas9^{D10A} nickase mice could also support *in vivo* gene editing studies aiming to dissect SSB repair mechanisms and model disease mutations in various tissues.

Limitations of the study

Despite its advances, our study has several limitations. Low residual indel frequencies persisted under spacer-nick conditions, which might be attributed to constitutive expression of Cas9^{D10A} nickase and prior activation of the cells to support HDR-mediated DNA donor template integration. The frequency of these residual indels in mouse hematopoietic cells was higher than that observed in human cells that were targeted with Cas9^{D10A} ribonucleoproteins (RNPs).[25] Other factors that may explain some of the observed differences between mouse and human HSPCs are variations in DNA repair activity and the intracellular dose of the Cas9^{D10A} endonuclease. Transgenic expression in mice likely results in a higher number of active Cas9^{D10A}-sgRNA RNP complexes compared with human cells, where RNPs are transiently introduced by electroporation. Increased and sustained exposure to nickase activity could enhance DNA nicking and elevate the chance that SSBs convert into DSBs if cells enter division before repair is completed. Because the *in-vitro*-edited cells were not synchronized for the cell cycle, nicked DNA might remain unrepaired until replication occurs, leading to low-frequency, unintended indels. Moreover, the kinetics of RNP assembly and persistence at target sites in Cas9^{D10A} nickase-transgenic cells remain untested. Variations in sgRNA sequence, strand orientation, and differential HDR activity between leading and lagging strands could contribute to the locus- and cell type-specific editing efficiencies observed with spacer-nick treatment. Two cancer-associated mutations (*Cd79b*-Y195H and *Notch1*-P2514*fs4) were introduced as examples but have not been studied further *in vivo* in this work. Expanding the system to a wider set of pathogenic mutations or to other tissue types beyond the hematopoietic lineage will further establish its general utility.

RESOURCE AVAILABILITY

Lead contact

Requests for further information and resources should be directed to the lead contact, Ralf Kühn (ralf.kuehn@mdc-berlin.de).

Materials availability

The *Rosa26-Cas9^{D10A}iresEGFP* mouse line generated in this study will be deposited to the Jackson Laboratory. The mouse line and all unique/stable reagents generated in this study are available from the lead contact, with a completed materials transfer agreement (MTA).

Data and code availability

Any additional information required to reanalyze the data reported in this paper is available from the lead contact upon request.

ACKNOWLEDGMENTS

We thank our colleagues Claudia Salomon, Sarina Hilke, Giuseppe Natale, and Jenniffer Pempe for excellent technical support. We thank Hans-Peter Rahn and Kirstin Rautenberg for assistance in the FACS core facility. We thank the staff in the animal and transgenics core facilities for excellent help with this project. This work was supported by the DFG (CH 1968/1-1) to V.T.C., the MGC Foundation to K.R., and by the Helmholtz Association, Zukunftsthema "Immunology & Inflammation" (ZT-0027) to K.R.

AUTHOR CONTRIBUTIONS

V.T.C., K.R., and J.T. conceptualized the study and led the project administration.V.T.C., R.K., and J.T. produced the Cas9^{D10A} nickase mouse strain. V.T.C., R.K., and J.T. developed and designed the methodology. J.T., V.T.C., D.B., and C.F.D. curated data. J.T. performed formal analyses. J.T. wrote the original manuscript draft. J.T., V.T.C., R.K., and K.R. reviewed and edited the manuscript. All authors approved the final manuscript. K.R. acquired funding.

Figure 3. Precise insertion of cancer-associated Y195H *Cd79b* and P2514*fs4 *Notch1* mutations into Cas9^{D10A} HSPCs

(A and B) Schematic of the CD79B (A) and Notch1 (B) protein sequences showing the positions of the Y195H and P2514*fs4 mutation hotspots in human and mouse.

(C and D) Schematic of the editing strategy of the mouse *Cd79b* (C) and *Notch1* (D) loci, respectively. The locations of sgRNA target sites (black arrows), rAAV donor homology arms, and PCR strategy to validate genome editing outcomes are indicated.

(E and F) Schematics presenting the *Cd79b* (E) and *Notch1* (F) editing approaches: double-strand break (DSB) in Cas9^{WT}-transgenic cells (left), and single-strand break (SSB) in Cas9^{D10A} nickase-transgenic cells for single-nick (middle) and spacer-nick (right).

(G and H) Quantification of HDR (left) and NHEJ (right) frequencies in the *Cd79b* (G) and *Notch1* (H) loci from HSPCs, respectively, assessed by amplicon NGS.

(I and J) HDR/NHEJ ratio for the *Cd79b* (I) and *Notch1* (J) loci in HSPCs. Data were pooled from 2–3 independent experiments and are represented as mean ± SD. Each symbol represents one mouse. Statistical analyses compared each group to Cas9^{WT}, using a two-tailed Mann-Whitney *U* test. *p* values are shown for comparisons reaching $p < 0.05$; all other comparisons were performed but did not reach statistical significance (see also Table S1).

See also Figures S4 and S5.

CellPress
OPEN ACCESS

Cell Reports Methods
Report

DECLARATION OF INTERESTS

J.T. is also currently affiliated with the Department of Pathology and Laboratory Medicine at Memorial-Sloan-Kettering Cancer Center, New York, United States of America. The "spacer-nick technology" is patented under the European Patent Application: EP21192657.1 (EP4392557A1).

STAR★METHODS

Detailed methods are provided in the online version of this paper and include the following:

- KEY RESOURCES TABLE
- EXPERIMENTAL MODEL AND STUDY PARTICIPANT DETAILS
  - Mice
  - Screening of F1 pups
  - Cell lines
- METHOD DETAILS
  - sgRNA design
  - RFLP assays
  - Cell culture and stimulation
  - sgRNA electroporation and AAV infection
  - Western blot
  - Flow cytometry
  - Genomic extraction, PCR, T7EI assay, ICE analysis and sanger sequencing
  - Sample preparation for amplicon NGS
  - Parameters for CRISPResso2 analysis
  - Off-target analysis
- QUANTIFICATION AND STATISTICAL ANALYSIS

SUPPLEMENTAL INFORMATION

Supplemental information can be found online at https://doi.org/10.1016/j.crmeth.2026.101668.

Received: July 14, 2026
Revised: September 17, 2026
Accepted: October 22, 2026

REFERENCES

1. Jinek, M., Chylinski, K., Fonfara, I., Hauer, M., Doudna, J.A., and Charpentier, E. (2012). A programmable dual-RNA-guided DNA endonuclease in adaptive bacterial immunity. Science *337*, 816–821. https://doi.org/10.1126/science.1225829.
2. Gasiunas, G., Barrangou, R., Horvath, P., and Siksnys, V. (2012). Cas9-crRNA ribonucleoprotein complex mediates specific DNA cleavage for adaptive immunity in bacteria. Proc. Natl. Acad. Sci. USA *109*, E2579–E2586. https://doi.org/10.1073/pnas.1208507109.
3. Cong, L., Ran, F.A., Cox, D., Lin, S., Barretto, R., Habib, N., Hsu, P.D., Wu, X., Jiang, W., Marraffini, L.A., and Zhang, F. (2013). Multiplex genome engineering using CRISPR/Cas systems. Science *339*, 819–823. https://doi.org/10.1126/science.1231143.
4. Mali, P., Esvelt, K.M., and Church, G.M. (2013). Cas9 as a versatile tool for engineering biology. Nat. Methods *10*, 957–963. https://doi.org/10.1038/nmeth.2649.
5. Cradick, T.J., Fine, E.J., Antico, C.J., and Bao, G. (2013). CRISPR/Cas9 systems targeting β-globin and CCR5 genes have substantial off-target activity. Nucleic Acids Res. *41*, 9584–9592. https://doi.org/10.1093/nar/gkt714.
6. Fu, Y., Foden, J.A., Khayter, C., Maeder, M.L., Reyon, D., Joung, J.K., and Sander, J.D. (2013). High-frequency off-target mutagenesis induced by CRISPR-Cas nucleases in human cells. Nat. Biotechnol. *31*, 822–826. https://doi.org/10.1038/nbt.2623.
7. Hsu, P.D., Scott, D.A., Weinstein, J.A., Ran, F.A., Konermann, S., Agarwala, V., Li, Y., Fine, E.J., Wu, X., Shalem, O., et al. (2013). DNA targeting specificity of RNA-guided Cas9 nucleases. Nat. Biotechnol. *31*, 827–832. https://doi.org/10.1038/nbt.2647.
8. Frock, R.L., Hu, J., Meyers, R.M., Ho, Y.J., Kii, E., and Alt, F.W. (2015). Genome-wide detection of DNA double-stranded breaks induced by engineered nucleases. Nat. Biotechnol. *33*, 179–186. https://doi.org/10.1038/nbt.3101.
9. Symington, L.S., and Gautier, J. (2011). Double-strand break end resection and repair pathway choice. Annu. Rev. Genet. *45*, 247–271. https://doi.org/10.1146/annurev-genet-110410-132435.
10. Symington, L.S. (2014). End resection at double-strand breaks: mechanism and regulation. Cold Spring Harbor Perspect. Biol. *6*, a016436. https://doi.org/10.1101/cshperspect.a016436.
11. Cho, S.W., Kim, S., Kim, Y., Kweon, J., Kim, H.S., Bae, S., and Kim, J.S. (2014). Analysis of off-target effects of CRISPR/Cas-derived RNA-guided endonucleases and nickases. Genome Res. *24*, 132–141. https://doi.org/10.1101/gr.162339.113.
12. Fu, Y., Sander, J.D., Reyon, D., Cascio, V.M., and Joung, J.K. (2014). Improving CRISPR-Cas nuclease specificity using truncated guide RNAs. Nat. Biotechnol. *32*, 279–284. https://doi.org/10.1038/nbt.2808.
13. Kleinstiver, B.P., Pattanayak, V., Prew, M.S., Tsai, S.Q., Nguyen, N.T., Zheng, Z., and Joung, J.K. (2016). High-fidelity CRISPR-Cas9 nucleases with no detectable genome-wide off-target effects. Nature *529*, 490–495. https://doi.org/10.1038/nature16526.
14. Slaymaker, I.M., Gao, L., Zetsche, B., Scott, D.A., Yan, W.X., and Zhang, F. (2016). Rationally engineered Cas9 nucleases with improved specificity. Science *351*, 84–88. https://doi.org/10.1126/science.aad5227.
15. Mali, P., Yang, L., Esvelt, K.M., Aach, J., Guell, M., DiCarlo, J.E., Norville, J.E., and Church, G.M. (2013). Rna-guided human genome engineering via cas9. Science *339*, 823–826. https://doi.org/10.1126/science.1232033.
16. Caldecott, K.W. (2008). Single-strand break repair and genetic disease. Nat. Rev. Genet. *9*, 619–631. https://doi.org/10.1038/nrg2380.
17. Dianov, G.L., and Hübscher, U. (2013). Mammalian base excision repair: the forgotten archangel. Nucleic Acids Res. *41*, 3483–3490. https://doi.org/10.1093/nar/gkt076.
18. Ran, F.A., Hsu, P.D., Wright, J., Agarwala, V., Scott, D.A., and Zhang, F. (2013). Genome engineering using the CRISPR-Cas9 system. Nat. Protoc. *8*, 2281–2308. https://doi.org/10.1038/nprot.2013.143.
19. Li, P.P., and Margolis, R.L. (2021). Use of single guided Cas9 nickase to facilitate precise and efficient genome editing in human iPSCs. Sci. Rep. *11*, 9865. https://doi.org/10.1038/s41598-021-89312-2.
20. Ran, F.A., Hsu, P.D., Lin, C.Y., Gootenberg, J., Konermann, S., Trevino, A.E., Scott, D., Inoue, A., Matoba, S., Zhang, Y., and Zhang, F. (2013). Double nicking by rna-guided crispr cas9 for enhanced genome editing specificity. Cell *154*, 1380–1389. https://doi.org/10.1016/j.cell.2013.08.021.
21. Mali, P., Aach, J., Stranges, P.B., Esvelt, K.M., Moosburner, M., Kosuri, S., Yang, L., and Church, G.M. (2013). CAS9 transcriptional activators for target specificity screening and paired nickases for cooperative genome engineering. Nat. Biotechnol. *31*, 833–838. https://doi.org/10.1038/nbt.2675.
22. Chu, V.T., Weber, T., Graf, R., Sommermann, T., Petsch, K., Sack, U., Volchkov, P., Rajewsky, K., and Kühn, R. (2016). Efficient generation of Rosa26 knock-in mice using CRISPR/Cas9 in C57BL/6 zygotes. BMC Biotechnol. *16*, 4. https://doi.org/10.1186/s12896-016-0234-4.
23. Platt, R.J., Chen, S., Zhou, Y., Yim, M.J., Swiech, L., Kempton, H.R., Dahlman, J., Parnas, O., Eisenhaure, T., Jovanovic, M., et al. (2014). CRISPR-Cas9 Knockin Mice for Genome Editing and Cancer Modeling. Cell *159*, 440–455. https://doi.org/10.1016/j.cell.2014.09.014.
24. Dow, L.E., Fisher, J., O'Rourke, K.P., Muley, A., Kastenhuber, E.R., Livshits, G., Tschaharganeh, D.F., Socci, N.D., and Lowe, S.W. (2015).

Please cite this article in press as: Trombke et al., A Cas9^{D10A} nickase mouse line for precise genome editing, Cell Reports Methods (2026), https://doi.org/10.1016/j.crmeth.2026.101668

Inducible in vivo genome editing with CRISPR-Cas9. Nat. Biotechnol. *33*, 390–394. https://doi.org/10.1038/nbt.3155.

25. Tran, N.T., Danner, E., Li, X., Graf, R., Lebedin, M., de la Rosa, K., Kühn, R., Rajewsky, K., and Chu, V.T. (2022). Precise CRISPR-Cas–mediated gene repair with minimal off-target and unintended on-target mutations in human hematopoietic stem cells. Sci. Adv. *8*, eabm9106. https://doi.org/10.1126/sciadv.abm9106.
26. Wefers, B., Bashir, S., Rossius, J., Wurst, W., and Kühn, R. (2017). Gene editing in mouse zygotes using the CRISPR/Cas9 system. Methods *121–122*, 55–67. https://doi.org/10.1016/j.ymeth.2017.02.008.
27. Wefers, B., Wurst, W., and Kühn, R. (2023). Gene editing in mouse zygotes using the crispr/cas9 system. Methods Mol. Biol. *2631*, 207–230. https://doi.org/10.1007/978-1-0716-2990-1_8.
28. Tran, N.T., Sommermann, T., Graf, R., Trombke, J., Pempe, J., Petsch, K., Kühn, R., Rajewsky, K., and Chu, V.T. (2019). Efficient crispr/cas9-mediated gene knockin in mouse hematopoietic stem and progenitor cells. Cell Rep. *28*, 3510–3522.e5. https://doi.org/10.1016/j.celrep.2019.08.065.
29. Tran, N.T., Trombke, J., Rajewsky, K., and Chu, V.T. (2020). Protocol for efficient crispr/cas9/aav-mediated homologous recombination in mouse hematopoietic stem and progenitor cells. STAR Protoc. *1*, 100028. https://doi.org/10.1016/j.xpro.2020.100028.
30. Young, R.M., Phelan, J.D., Wilson, W.H., and Staudt, L.M. (2019). Pathogenic B-cell receptor signaling in lymphoid malignancies: New insights to improve treatment. Immunol. Rev. *291*, 190–213. https://doi.org/10.1111/imr.12792.
31. Takeuchi, T., Yamaguchi, M., Kobayashi, K., Miyazaki, K., Imai, H., Ono, R., Tawara, I., Nosaka, T., Tanaka, K., and Katayama, N. (2016). Myd88, cd79b, and cd79a gene mutations in cd5-positive diffuse large b-cell lymphoma. Blood *128*, 1861. https://doi.org/10.1002/cncr.30404.
32. Kraan, W., Horlings, H.M., van Keimpema, M., Schilder-Tol, E.J.M., Oud, M.E.C.M., Scheepstra, C., Kluin, P.M., Kersten, M.J., Spaargaren, M., and Pals, S.T. (2013). High prevalence of oncogenic MYD88 and CD79B mutations in diffuse large B-cell lymphomas presenting at immune-privileged sites. Blood Cancer J. *3*, e139. https://doi.org/10.1038/bcj.2013.28.
33. Puente, X.S., Pinyol, M., Quesada, V., Conde, L., Ordóñez, G.R., Villamor, N., Escaramis, G., Jares, P., Beà, S., González-Díaz, M., et al. (2011). Whole-genome sequencing identifies recurrent mutations in chronic lymphocytic leukaemia. Nature *475*, 101–105. https://doi.org/10.1038/nature10113.
34. Fabbri, G., Rasi, S., Rossi, D., Trifonov, V., Khiabanian, H., Ma, J., Grunn, A., Fangazio, M., Capello, D., Monti, S., et al. (2011). Analysis of the chronic lymphocytic leukemia coding genome: role of NOTCH1 mutational activation. J. Exp. Med. *208*, 1389–1401. https://doi.org/10.1084/jem.20110921.
35. Rossi, D., Rasi, S., Fabbri, G., Spina, V., Fangazio, M., Forconi, F., Marasca, R., Laurenti, L., Bruscaggin, A., Cerri, M., et al. (2012). Mutations of NOTCH1 are an independent predictor of survival in chronic lymphocytic leukemia. Blood *119*, 521–529. https://doi.org/10.1182/blood-2011-09-379966.
36. Wang, Y., Du, Y., Shen, B., Zhou, X., Li, J., Liu, Y., Wang, J., Zhou, J., Hu, B., Kang, N., et al. (2015). Efficient generation of gene-modified pigs via injection of zygote with Cas9/sgRNA. Sci. Rep. *5*, 8256. https://doi.org/10.1038/srep08256.
37. Whitworth, K.M., Benne, J.A., Spate, L.D., Murphy, S.L., Samuel, M.S., Murphy, C.N., Richt, J.A., Walters, E., Prather, R.S., and Wells, K.D. (2017). Zygote injection of CRISPR/Cas9 RNA successfully modifies the target gene without delaying blastocyst development or altering the sex ratio in pigs. Transgenic Res. *26*, 97–107. https://doi.org/10.1007/s11248-016-9989-6.
38. Teixeira, M., Py, B.F., Bosc, C., Laubreton, D., Moutin, M.J., Marvel, J., Flamant, F., and Markossian, S. (2018). Electroporation of mice zygotes with dual guide RNA/Cas9 complexes for simple and efficient cloning-free genome editing. Sci. Rep. *8*, 474. https://doi.org/10.1038/s41598-017-18826-5.
39. Takemoto, T. (2020). Zygote electroporation for crispr/cas9 delivery to generate genetically modified mice. In Electroporation Protocols: Microorganism, Mammalian System, and Nanodevice, S. Li, L. Chang, and J. Teissie, eds. (Springer US), pp. 121–126. https://doi.org/10.1007/978-1-4939-9740-4_13.
40. Komor, A.C., Kim, Y.B., Packer, M.S., Zuris, J.A., and Liu, D.R. (2016). Programmable editing of a target base in genomic DNA without double-stranded DNA cleavage. Nature *533*, 420–424. https://doi.org/10.1038/nature17946.
41. Gaudelli, N.M., Komor, A.C., Rees, H.A., Packer, M.S., Badran, A.H., Bryson, D.I., and Liu, D.R. (2017). Programmable base editing of a · t to g · c in genomic dna without dna cleavage. Nature *551*, 464–471. https://doi.org/10.1038/nature24644.
42. Huang, T.P., Newby, G.A., and Liu, D.R. (2021). Precision genome editing using cytosine and adenine base editors in mammalian cells. Nat. Protoc. *16*, 1089–1128. https://doi.org/10.1038/s41596-020-00450-9.
43. Yin, H., Xue, W., Chen, S., Bogorad, R.L., Benedetti, E., Grompe, M., Koteliansky, V., Sharp, P.A., Jacks, T., and Anderson, D.G. (2014). Genome editing with Cas9 in adult mice corrects a disease mutation and phenotype. Nat. Biotechnol. *32*, 551–553. https://doi.org/10.1038/nbt.2884.
44. Mikuni, T., Nishiyama, J., Sun, Y., Kamasawa, N., and Yasuda, R. (2016). High-Throughput, High-Resolution Mapping of Protein Localization in Mammalian Brain by In Vivo Genome Editing. Cell *165*, 1803–1817. https://doi.org/10.1016/j.cell.2016.04.044.
45. Yang, Y., Wang, L., Bell, P., McMenamin, D., He, Z., White, J., Yu, H., Xu, C., Morizono, H., Musunuru, K., et al. (2016). A dual AAV system enables the Cas9-mediated correction of a metabolic liver disease in newborn mice. Nat. Biotechnol. *34*, 334–338. https://doi.org/10.1038/nbt.3469.
46. Nojima, T., Haniuda, K., Moutai, T., Matsudaira, M., Mizokawa, S., Shiratori, I., Azuma, T., and Kitamura, D. (2011). In-vitro derived germinal centre B cells differentially generate memory B or plasma cells in vivo. Nat. Commun. *2*, 465. https://doi.org/10.1038/ncomms1475.
47. Trombke, J. (2024). Modeling Human Lymphoid Malignancies by CRISPR/Cas9-mediated Mutagenesis in the Notch1 PEST Domain of Mouse Hematopoietic Stem and Progenitor Cells (FU Berlin Refubium). https://doi.org/10.17169/refubium-47234.
48. Chu, V.T., Graf, R., Wirtz, T., Weber, T., Favret, J., Li, X., Petsch, K., Tran, N.T., Sieweke, M.H., Berek, C., et al. (2016). Efficient CRISPR-mediated mutagenesis in primary immune cells using CrispRGold and a C57BL/6 Cas9 transgenic mouse line. Proc. Natl. Acad. Sci. USA, 12514–1251412519. https://doi.org/10.1073/pnas.1613884113.
49. Conant, D., Hsiau, T., Rossi, N., Oki, J., Maures, T., Waite, K., Yang, J., Joshi, S., Kelso, R., Holden, K., et al. (2022). Inference of Crispr Edits from Sanger Trace Data. Bioinformatics *5*, 123–130. https://doi.org/10.1089/crispr.2021.0113.
50. Clement, K., Rees, H., Canver, M.C., Gehrke, J.M., Farouni, R., Hsu, J.Y., Cole, M.A., Liu, D.R., Joung, J.K., Bauer, D.E., and Pinello, L. (2019). CRISPResso2 provides accurate and rapid genome editing sequence analysis. Nat. Biotechnol. *37*, 224–226. https://doi.org/10.1038/s41587-019-0032-3.

Please cite this article in press as: Trombke et al., A Cas9^{D10A} nickase mouse line for precise genome editing, Cell Reports Methods (2026), https://doi.org/10.1016/j.crmeth.2026.101668

STAR★METHODS

KEY RESOURCES TABLE

REAGENT or RESOURCE	SOURCE	IDENTIFIER
Antibodies		
TrueStain FcX™ (anti-mouse CD16/32, clone 93)	BioLegend	Cat# 101320; RRID: AB_1574973
BV785 anti-mouse Ly6A/E (Sca1) (clone D7)	BioLegend	Cat# 108139; RRID: AB_2565957
APC anti-mouse CD117 (c-Kit) (clone 2B8)	BioLegend	Cat# 105812; RRID: AB_313221
APC/Cy7 anti-mouse CD48 (clone HM48-1)	BioLegend	Cat# 103431; RRID: AB_2561462
BV605 anti-mouse CD150 (clone TC15-12F12.2)	BioLegend	Cat# 115927; RRID: AB_11204248
PE/Cy7 anti-mouse B220 (clone RA3-6B2)	BioLegend	Cat# 103221; RRID: AB_313004
PE/Cy7 anti-mouse CD3e (clone 145-2C11)	BioLegend	Cat# 100319; RRID: AB_312684
PE/Cy7 anti-mouse Gr-1 (clone RB6-8C5)	BioLegend	Cat# 108415; RRID: AB_313380
PE/Cy7 anti-mouse Ter-119 (clone TER-119)	BioLegend	Cat# 116221; RRID: AB_2137789
PE/Cy7 anti-mouse CD11b (clone M1/70)	BioLegend	Cat# 101215; RRID: AB_312798
PE/Cy7 anti-mouse CD11c (clone N418)	BioLegend	Cat# 117317; RRID: AB_493569
BV785 anti-mouse CD19 (clone 6D5)	BioLegend	Cat# 115543; RRID: AB_11218994
A647 anti-mouse CD3 (clone145-2C11)	BioLegend	Cat# 100322; RRID: AB_389322
PE/Cy7 anti-mouse NK1.1 (clone PK136)	BioLegend	Cat# 108713; RRID: AB_389363
A700 anti-mouse Gr-1 (RB6-8C5)	BioLegend	Cat# 108421; RRID: AB_493728
BV605 anti-mouse CD11b (M1/70)	BioLegend	Cat# 101237; RRID: AB_11126744
PE anti-mouse CD11c (clone N418)	BioLegend	Cat# 117307; RRID: AB_313776
BV785 anti-mouse B220 (clone RA3-6B2)	BioLegend	Cat# 103246; RRID: AB_2563256
BV605 anti-mouse CD19 (clone 6D5)	BioLegend	Cat# 115540; RRID: AB_2563067
PE/Cy7 anti-mouse Fas (CD95) (clone Jo2)	BD Biosciences	Cat# 557653; RRID: AB_396768
A700 anti-mouse CD38 (clone 90)	eBioscience	Cat# 56-0381-82; RRID: AB_657740
PE anti-mouse IgG1 (clone A85-1)	BD Biosciences	Cat# 550083; RRID: AB_393553
APC anti-mouse CD43 (clone S7)	BD Biosciences	Cat# 560663; RRID: AB_1727479
PE anti-mouse CD5 (clone 53-7.3)	BioLegend	Cat# 100608; RRID: AB_312737
PE/Cy7 anti-mouse IgM (clone II/41)	Invitrogen	Cat# 25-5790-82; RRID: AB_469655
BV510 anti-mouse CD44 (clone IM7)	BioLegend	Cat# 103044; RRID: AB_2650923
APC anti-mouse CD25 (clone PC61)	BioLegend	Cat# 102012; RRID: AB_312861
PerCpCy5.5 anti-mouse CD8a (clone 53-6.7)	BioLegend	Cat# 100733; RRID: AB_2075239
BV7411 anti-mouse CD4 (clone RM4-5)	BioLegend	Cat# 100550; RRID: AB_2562099
Cas9 (S. pyogenes) (clone 7A9-3A3) Mouse mAb	Cell Signaling	Cat# 14697S; RRID: AB_2750916
β-Actin (clone AC-74) Mouse mAb	Sigma Aldrich	Cat# A2228; RRID: AB_476697
Goat anti-mouse IgG1-HRP	Southern Biotech	Cat# 1070-05; RRID: AB_2650509
Armenian Hamster anti-mouse CD40 mAb, Unconjugated, (clone HM40-3)	BD Biosciences	Cat# 553721; RRID: AB_395006
Bacterial and virus strains		
TOP10	Invitrogen	Cat# C404003
AAV-6	Cell Biolabs	Cat#VPK-410-SER6
Biological samples		
Mouse primary cells	MDC Berlin, Germany	N/A

(*Continued on next page*)

Please cite this article in press as: Trombke et al., A Cas9^{D10A} nickase mouse line for precise genome editing, Cell Reports Methods (2026), https://doi.org/10.1016/j.crmeth.2026.101668

Continued

REAGENT or RESOURCE	SOURCE	IDENTIFIER
Chemicals, peptides, and recombinant proteins		
Alt-R®CRISPR-Cas9 tracrRNA, 100nmol	IDT	Cat# 1072534
4′,6-diamidino-2-phenylindole	Sigma Aldrich	Cat# D9542
Sodium azide (NaN3)	Sigma Aldrich	Cat# S8032-25G
Sodium chloride (NaCl)	Carl Roth	Cat# 3957.2
DOC (sodium deoxycholate)	Sigma Aldrich	Cat# D6/50-25G
Trysin-EDTA	Sigma	Cat# T3924-100mL
Beta-Mercaptoethanol (52mM)	Sigma	Cat# M3148-250ML
Tris base	Carl Roth	Cat# 5429.2
Tris-HCL	Roth	Cat# 9090.3
Potassium chloride (KCl)	Sigma Aldrich	Cat# 60128
Ethylenediaminetetraacetic acid (EDTA)	Carl Roth	Cat# 8040.2
Sodium succinate (C4H4Na2O4)	SERVA	Cat# 14972
Sodium phosphate dibasic (Na2HPO4)	Sigma Aldrich	Cat# S7907
Potassium bicarbonate (KHCO3)	Sigma Aldrich	Cat# 237205
Magnesium chloride (MgCl2)	Roth	Cat# KK36.3
NP-40	Thermo Fisher	Cat# J60766.AK
Tween 20	Sigma	Cat# P6585-10ML
Proteinase K (for ear clip lysis buffer)	Qiagen	Cat# RP100B
SDS	Sigma	Cat# 428029
Protease Inhibitors	Sigma	Cat# 05892791001
99% Ethanol	MDC Berlin, Germany	N/A
Methanol	Chemsolute	Cat# CSO.1437.2500.PB
StemSpan™ SFEM II	StemCell	Cat# 09655
DMEM$^{+/+}$	Gibco	Cat# 41966052
1M HEPES	Gibco	Cat# 15630056
Non-Essential Animo Acids (NEAA)	Gibco	Cat# 11140050
PBS pH7.2	Gibco	Cat# 20012019
BSA, Albumin Fraction V	Carl Roth	Cat# 8076.3
FBS	Sigma Aldrich	Cat# F7524-500mL
Trysin-EDTA	Gibco	Cat# 10779417
Gentamycin	Lonza	Cat# 17-519L
Mouse recombinant TPO	Peprotech	Cat# 315-14
Mouse recombinant SCF	Peprotech	Cat# 250-03
Mouse recombinant Flt3-ligand	Peprotech	Cat# 250-31L
Human recombinant IL-11	Peprotech	Cat# 200-11
Mouse recombinant IL-2	R&D	Cat# 402-ML-020/CF
Mouse recombinant IL-4	Peprotech	Cat# 214-14
Mouse CD3/CD28 DynaBeads	Invitrogen	Cat# 11452D
Quick Extract™ DNA Extraction Solution 1.0	Lucigen	Cat# QE09050
10% SDS Gels	Biorad	Cat# 4561033EDU
PVDF membranes	Thermo Fisher	Cat# 88520
ECL™ Prime Western-Blot-System	Sigma Aldrich	Cat# GERPN2232
Midori Green	Nippon Genetics Europe GmBH	Cat# K1820-01
Agarose	Biozym	Cat# 840040
Gene Ruler 1Kb Plus Leddar	Life Technologies	Cat# SM1332
Milk Powder	Fluka	Cat# 70166-500G
Protein extraction beads	Diagenode	Cat# C20000021

(*Continued on next page*)

Please cite this article in press as: Trombke et al., A Cas9^{D10A} nickase mouse line for precise genome editing, Cell Reports Methods (2026), https://doi.org/10.1016/j.crmeth.2026.101668

Continued

REAGENT or RESOURCE	SOURCE	IDENTIFIER
Critical commercial assays		
Anti-mouse Sca1 MicroBead Kit (VioBright™ FITC)	Miltenyi Biotec	Cat# 130-123-124
Anti-mouse CD43 (Ly48) MicroBead Kit	Miltenyi Biotec	Cat# 130-049-801
PrimeSTAR® GXL DNA Polymerase	TaKaRa	Cat# R050B
Herculase II Fusion DNA Polymerase	Agilent Technology	Cat# 600677
DreamTaq PCR Master Mixes (2×)	Thermo Fischer	Cat# K1082
p.JET TOPO cloning Kit	Thermo Fischer	Cat# K1231
T7 endonuclease I	NEB	Cat# M0302S
TaqMan Universal PCR MasterMix	Applied Biosystems	Cat# 4324018
NucleoSpin Gel and PCR Clean up	Macherey-Nagel	Cat# 740609.250
NucleoSpin Plasmid, Mini kit for plasmid DNA	Macherey-Nagel	Cat# 740588.250
AMPure XP beads	Beckman Coulter	Cat# A63880
Qubit dsDNA HS assay kit	Invitrogen	Cat# Q33230
Experimental Models: Cell Lines		
40LB Feeder cells	Nojima et al.,[46]	N/A
Experimental models: Organisms/strains		
C57BL/6N	Charles River, Sulzbach, Germany	N/A
NMRI	Charles River, Sulzbach, Germany	N/A
R26-Cas9iEGFP mice: B6(C)-Gt(ROSA)26Sorem1.1(CAG-cas9*,-EGFP)Rsky/J (Strain #:028555)	Chu et al., 2016[22]; The Jackson Laboratory	RRID: IMSR_JAX:028555
R26-Cas9D10AiEGFP mice	This paper	N/A
Recombinant DNA		
AAV-6 Rep/Cap plasmid	Cell Biolabs	Cat# VPK-426
AAV-helper plasmid	Cell Biolabs	Cat# VPK-400-DJ
AAV-GFP genome plasmid	Cell Biolabs	Cat# AAV-400
pAAV-LaminB1-mCherry	Tran et al., 2019[29]	N/A
pAAV-CD79B-Y196H	This paper	N/A
pAAV-Notch1-P2514*fs4	Trombke, 2024[47]	https://doi.org/10.17169/refubium-47234
pAAV-Notch1-P2514*fs4-mCherry	Trombke, 2024[47]	https://doi.org/10.17169/refubium-47234
Software and algorithms		
FlowJo v10	BD Biosciences	https://www.flowjo.com/
CrispRGold	Chu et al.,[48]	https://crisprgold.mdc-berlin.de
Fiji/ImageJ	ImageJ	https://imagej.net/software/fiji/
Interference of CRISPR edits (ICE)	Hsiau et al.,[49]	https://ice.synthego.com/
CRISPRESSO v2	Clement et al.,[50]	http://crispresso2.pinellolab.org/
Graphpad Prism v10	GraphPad Software	https://www.graphpad.com/
Other		
Amaxa 4D Nucleofector	Lonza	N/A
16-well Nucleocuvette™ Strips	Lonza	Cat# V4XP-3032
BD Filcon, Sterile, Cup-Type	BD Biosciences	Cat# 340629
50mL Polystyrene Conical Tube	Corning	Cat# 352070
15mL Polystyrene Conical Tube	Corning	Cat# 352096
0.45µm PES filter	Jet Biofill	Cat# FCA-406-030
0.22µm PES filter small	Santa Cruz Biotechnology	Cat# Sc-516079
0.22µm PES filter	Whatman Life Sciences	Cat# 10462200
50µm Filter mesh	BD	Cat# 340632

(*Continued on next page*)

Cell Reports Methods
Report

CellPress
OPEN ACCESS

Continued

REAGENT or RESOURCE	SOURCE	IDENTIFIER
2,10 × 80mm 14G x 3 1/8″ needle	Braun	Cat# 4665473
1,2 × 38mm 18Gx 1 ½'' needle	Terumo®	Cat# AN*1838S1
0,9 × 40mm 20G 1 ½'' needle	Braun	Cat# 4657519
0,5 × 16mm 25G 5/8″ needle	Henry Schein®	Cat# 9003629
0,4 × 19mm 27G 1 ½'' needle	BD	Cat# 302200
1mL syringe	Braun	Cat# 9161406V
5mL syringe	Braun	Cat# 4606051V
10mL syringe	Braun	Cat# 4606108V
20mL syringe	Braun	Cat# 4606205V
Kimwipe Tissue	Kimwipe	Cat# 7552
Cell Scraper 245 mm length	Carl Roth	Cat# EKX9.1
LS Columns	Miltenyi Biotec	Cat# 130-042-401
MS Columns	Miltenyi Biotec	Cat# 130-042-201

EXPERIMENTAL MODEL AND STUDY PARTICIPANT DETAILS

Mice

Generation of the Rosa26-Cas9^{D10A}iresEGFP *mice*

Cas9^{D10A} transgenic mice were generated by CRISPR/Cas9-mediated introduction of the D10A codon into the existing *Rosa26-Cas9iresEGFP* (R26-Cas9iEGFP) locus[22] through mouse zygote mutagenesis (Figure 1A). The original Cas9 and the recently developed Cas9^{D10A} transgene are both expressed from the *Rosa26* locus under the ubiquitous CAG promoter, and transgene expression is monitored by the expression of an FRT-flanked IRES-EGFP reporter. The FRT-flanked IRES-EGFP reporter gene can be deleted either by crossing the *Rosa26-Cas9D10AiresEGFP* mice with FLP-deleter mice (Jackson Laboratory Strain #011065), or by injecting Flippase recombinase mRNA into Rosa26-*Cas9D10AiresEGFP* zygotes to obtain a reporter-free Cas9^{D10A} mouse line. Seven sgRNAs flanking the codon encoding aspartic acid (D) at position 10 of the Cas9^{WT} protein were designed and screened for gene editing efficiency in Cas9-expressing B cells (Figures S1B and S1C). sgCas9-1 and sgCas9-2 with high gene editing efficiency (~80%) were selected for zygote editing. Zygotes obtained by mating male Cas9^{WT} and female C57BL/6 mice (Charles River, Sulzbach, Germany) were electroporated as previously described[26,27] with sgRNA2/Cas9 RNP complexes and the ssODN HDR donor template (Table S3). The ssODN HDR donor template included the D10A mutation, silent replacements that create a diagnostic KpnI restriction enzyme digestion site, allowing screening of Cas9D10A-positive offspring by PCR (Figures S1A–S1C), and 60 nt homology arms (Figure 1A). The electroporated zygotes were then transferred into pseudo-pregnant NMRI female mice to obtain mutant founder mice (Figure S1A). 7/54 offspring (12%) were positive for the D10A PCR product (Figure S1D). We then validated the positive pups by Sanger sequencing and found correct integration of the D10A mutation into the Cas9 allele in 3 of the 7 pups. Founder mice #R6685 (male) and R#6610 (female) were used to establish the Cas9^{D10A} transgenic mouse line (Figure S1E). Animals were handled according to institutional guidelines under experimental license number (G0051/22-E173) approved by the Landesamt für Gesundheit and Soziales (Berlin, Germany).

Screening of F1 pups

Genomic DNA was obtained from ear biopsies of F1 pups. 300 μL of lysis buffer (50 mM Tris (pH 8.0), 50 mM KCl, 2.5 mM EDTA (pH 8.0), 0.45% NP-40, 0.45% Tween 20 in water, supplemented with 5 μL Proteinase K (Qiagen)) was used to lyse each ear biopsy. Lysis was performed at 56°C overnight on a shaking platform. The ear biopsies were then boiled in lysis buffer at 80°C for 30 min. The targeted sequence in the Cas9 allele was amplified by PCR (DreamTaq, Thermo Fisher) using gene-specific primers (Table S3). PCR products from Cas9^{D10A} positive founders were cloned into pJET cloning vectors (Thermo Fisher) following the manufacturer's protocol. 96 single bacterial colonies were picked and subjected to Sanger sequencing (LGC Genomics, Berlin, Germany). Cas9^{D10A} transgenic founders were backcrossed to C57BL/6N animals (Charles River, Sulzbach, Germany), and the Cas9^{D10A} allele was kept in a heterozygous state.

Cell lines

40LB feeder cells were cultured as previously described.[46] In brief, 40LB cells were maintained in DMEM$^{+/+}$ supplemented with 10% FBS. One day before the edited B cell co-culture, 40LB feeder cells were harvested by trypsinization and plated at 5 × 10^4 cells/cm^2 per well in 12-well plates. On the day of B cell co-culture, 40LB plates were irradiated with 12 Gγ 4 h before the B cell transfer.

Please cite this article in press as: Trombke et al., A Cas9^{D10A} nickase mouse line for precise genome editing, Cell Reports Methods (2026), https://doi.org/10.1016/j.crmeth.2026.101668

METHOD DETAILS

sgRNA design

sgRNAs were designed using CrispRGold Version 1.1 (https://crisprgold.mdc-berlin.de).[48] Spacer-nick sgRNA pairs flanking the target regions with varying spacer distances were designed in a PAM-out configuration. All sgRNAs were of high specificity, with the lowest off-target prediction score ≥6. All sgRNAs were purchased from IDT and are listed in Table S3.

RFLP assays

For RFLP assays, 200–300 ng of the purified PCR products using AMPure XP beads (Beckman Coulter) were digested with the restriction enzyme BssSI (Thermo Fisher) for 1 h at 37°C. Cleaved DNA fragments were separated on a 1.2% agarose gel, supplemented with Midori Green (Nippon Genetics Europe GmbH). The intensity of cleaved DNA bands was quantified using Fiji/ImageJ (NIH).

Cell culture and stimulation

For Sca1$^+$ cell stimulation, Sca1$^+$ cells were isolated from the bone marrow of Cas9^{WT} and Cas9^{D10A} mice using the Sca1 enrichment kit according to the manufacturer's protocol (Milteny Biotec). 1.5 × 10^5 Sca1$^+$ cells were cultured in 1 mL of serum-free StemSpan^{TM} SFEM II medium (Stem Cell Technologies) supplied with mouse SCF (50 ng/mL), mouse TPO (50 ng/mL), mouse Flt3L (50 ng/mL), and human IL-11 (50 ng/mL, all purchased from Peprotech) for 2 days in an incubator at 37°C and 5% CO_2.

For T cell activation, T cells were isolated from the spleen of Cas9^{WT} and Cas9^{D10A} mice using CD43 microbeads (Milteny Biotec, positive fraction). 1 × 10^6 cells/mL were cultured in DMEM$^{+/+}$ medium (Gibco) supplied with 10% FBS (Sigma-Aldrich), 2mM HEPES (Gibco), and 1× NEAA (Gibco), 52 mM beta-mercaptoethanol (Sigma), and stimulated with anti-CD3/CD28 DynaBeads (Invitrogen) according to the manufacturer's protocol and in the presence of 20 ng of mouse IL-2 (R&D) for 2 days.

For B cell activation, B cells were isolated from the spleen of Cas9^{WT} and Cas9^{D10A} mice using CD43 microbeads (Milteny Biotec, negative fraction). B cells were cultured in 1 × 10^6 cells/mL in DMEM$^{+/+}$ medium supplied with 10% FCS, 2mM HEPES, and 1× NEAA, 52 mM beta-mercaptoethanol, and stimulated with 5 μg of anti-CD40 (clone HM40-3, BD Biosciences) antibody and 20 ng of mouse IL-4 (Peprotech) for 2 days.

sgRNA electroporation and AAV infection

sgRNAs were generated by mixing 100 pmol of crRNA (IDT) and tracrRNA (IDT) in equal ratios, incubated at 95°C for 5 min, and cooled down to room temperature. sgRNA sequences are listed in Table S3. For sgRNA electroporation, 3 × 10^5 LSK cells and 1 × 10^6 B or T cells were electroporated with 100 pmol and 200 pmol of each sgRNA in 20 μL of AMAXA electroporation buffer (90 mM Na_2HPO_4, 5 mM KCL, 10 mM $MgCl_2$, 20 mM HEPES, 25 mM Sodium succinate in deionized water), respectively, using the DN-100 pulse for T cells, or the DI-100 pulse for B cells and LSK cells (Amaxa 4D Nucleofector, Lonza). After electroporation, cells were transferred to pre-warmed medium supplied with cytokines and rAAV-6 donor vectors (MOI of 5 × 10^6 GC/cell) that were produced as previously described.[29]

One day after electroporation, 50% of the medium was replaced for LSK and T cells. Two days after genome editing, LSK and T cells were purified by FACS. B cells were seeded on 40LB feeder cells (producing mouse CD40L and BAFF)[46] one day after genome editing in the presence of 20 ng/mL IL-4 (Peprotech) to keep them proliferating until three days post genome editing followed by FACS purification.

Western blot

Western Blot was performed with standard buffers. LSK cells of Cas9^{D10A} and Cas9^{WT-HET} mice derived from expansion cultures on day 2 (see above and[28,29]). T and B cells were isolated from spleens of Cas9^{D10A}, Cas9^{WT-HET} and Cas9^{WT-HOM} mice and left unstimulated. Cells were lysed in RIPA buffer (20 mM Tris-HCL (pH 7.5), 150 mM NaCl, 1% NP-40, 0.1% SDS, 0.1% Sodium deoxycholate, 1 mM EDTA) supplied with protease inhibitors (Sigma). Proteins were extracted from tissues using a Bioruptor^R sonicator according to the manufacturer's instructions (Diagenode). For SDS-PAGE, 30–200 μg of protein was loaded onto pre-cast gels (Bio-Rad). Electrophoresis was performed for 20–30 min at 80V and another 60 min at 120V. Proteins were wet-transferred to PVDF (Thermo Fisher) membranes overnight for 16 h at 60V on ice at 4°C. Membranes were blocked in 5% milk-containing TBST Buffer and incubated overnight in appropriate dilutions in 5% milk (Fluka) -containing TBST Buffer of mouse Cas9 and β-Actin antibodies at 4°C and HRP-coupled antibodies were incubated for 1 h at room temperature (see key resources table & Figure legends for details on the usage of Western Blot antibodies used in this study). Nitrocellulose membranes were developed using the ECL^{TM} Prime Western-Blot system (Sigma) and captured via chemical luminescence imaging.

Flow cytometry

For flow cytometric analysis, single cell suspensions were prepared from bone marrow, spleen, mesenteric lymph nodes, thymus and peritoneal cavity of C57BL/6, Cas9^{WT} and Cas9^{D10A} animals in FACS buffer (2% BSA, 0.09% NaN_3 in PBS). Erythrocytes were lysed for 5 min on ice using erythrocyte lysis buffer (155 mM NH_4Cl, 10 mM $KHCO_3$, 0.1 mM EDTA in deionized water). The reaction was stopped with FACS buffer. After 10 min blocking the Fc receptors with FcγR antibodies (Biolegend), the surface antigens were stained in 100 μL FACS buffer containing the fluorescent-conjugated antibodies (Biolegend or BD Bioscience; see key resources table & Figure legends for details on the usage of fluorescent antibodies used in this study) for 20 min and then washed 3 times

Please cite this article in press as: Trombke et al., A Cas9^{D10A} nickase mouse line for precise genome editing, Cell Reports Methods (2026), https://doi.org/10.1016/j.crmeth.2026.101668

with FACS Buffer to remove residual antibodies. All antibodies were titrated prior for optimal performance. Cells were analyzed using the Fortessa BD analyzer. DAPI (200 ng/mL in FACS Buffer, Sigma-Aldrich) was used to exclude dead cells. Data analysis was performed using FlowJo® Version 10.

Genomic extraction, PCR, T7EI assay, ICE analysis and sanger sequencing

Genomic DNA from cell pellets was extracted using the QuickExtract DNA extraction kit following the manufacturer's protocol (Epicentre). The targeted sequences were amplified from genomic DNA by PCR using Herculase II Fusion DNA Polymerase (Agilent Technology) or PrimeSTAR GXL DNA Polymerase (TaKaRa) with gene-specific primers (see Table below). PCR products were cleaned up using AMPure XP beads (Beckman Coulter) or by gel electrophoresis and subsequent NucleoSpin Gel and PCR clean-up kit (Macherey-Nagel). For the T7 endonuclease I (T7EI) assay (NEB), PCR products were digested with T7EI for 60 min at 37°C, and cleaved DNA fragments were separated on 1.5% agarose gels (Biozym). The intensity of cleaved DNA bands was quantified using ImageJ (NIH) and the percentage of indels (cutting %) was calculated as previously described.[3] For ICE analysis (indel analysis), cleaned PCR products were sequenced using Sanger sequencing (LGC Genomics, Berlin Germany), and Indel frequencies were analyzed using the Interference of CRISPR edits (ICE) tool (Synthego).[49]

Sample preparation for amplicon NGS

To quantify WT, NHEJ, and HDR events at the targeted loci, we performed amplicon NGS (Genewiz, Leipzig, Germany). An external PCR was performed using PrimeSTAR GXL polymerase (TaKaRa) with external primers (Table S3) that anneal to a genomic sequence outside of the 5′ or 3′ homology arms to exclude contamination by the remaining AAV-6 HDR donor vectors in the sample. Primers marked in blue in Figure 2A (*Lmnb1* locus) and Figures 3C and 3D (*Cd79b* and *Notch1* loci) anneal outside of the homology arms, red primers in these Figures indicate primers for the nested PCR. The PCR was performed under the following PCR conditions: 98°C for 2 min; 25 cycles (98°C for 10 s, 60°C–62°C for 20 s, 68°C for 90 s) and 68°C for 2 min. PCR products were run on a 1.2% agarose (Biozym) gel, and bands were purified using the NucleoSpin Gel and PCR clean-up kit (Macherey-Nagel). A nested PCR was performed using Herculase II Fusion DNA Polymerase (Agilent Technologies) (*CD79B*) or PrimeSTAR GXL polymerase (Takara) (*Lmnb1, Notch1*) with nested primers (Table S3) annealing to sequences near Cas9 targeting sites. The nested PCR was performed with the following PCR conditions: 95°C for 2 min; 25 cycles (95°C for 20 s, 60°C–64°C for 20 s, 72°C for 30 s) and 72°C for 3 min. PCR products were cleaned using AMPure XP beads (Beckman Coulter) (*CD79B*) or by electrophoresis on 1.5% agarose gels (*Lmnb1 and Notch1*) and subsequent clean-up using the NucleoSpin Gel and PCR clean-up kit (Macherey-Nagel). DNA concentrations were normalized to 20 ng/μL using a Qubit dsDNA HS assay kit (Invitrogen) or NanoDrop. The amplicon libraries were sequenced using the MiSeq sequencing service provided by Genewiz Germany (www.genewiz.com). Amplicon data were analyzed using the CRISPResso2 tool[50] (http://crispresso2.pinellolab.org).

Parameters for CRISPResso2 analysis

In CRISPResso2 (http://crispresso2.pinellolab.org),[50] paired-end read analysis was performed. The amplicon reference and sgRNA sequences were entered. For Cas9^{D10A} single-nick and Cas9^{WT} samples, one sgRNA was entered, whereas Cas9^{D10A} spacer-nick and control samples were analyzed with the respective paired sgRNAs for *Lmnb1*, *CD79B,* or *Notch1*. In the optional parameters, 50% sequence homology (minimum) and a 50 bp quantification window size were set. 20 nucleotides (the primer sequences) were trimmed from the ends. Substitutions were excluded from the analysis as they may represent PCR or sequencing errors. Trimming of the Illumina adapters and filtering for read and base quality with a Phred score of 33 were performed by the sequencing company before results delivery.

Off-target analysis

Off-targets were predicted *in silico* with CrispRGold Version 1.1 (https://crisprgold.mdc-berlin.de)[48] (Table S2). PCR amplicon NGS was performed (Genewiz, Leipzig, Germany). Primer sequences are listed in Table S3. All PCRs were performed with GXL polymerase (TaKaRa) and optimized for optimal annealing temperature. PCRs were performed under the following conditions: 95°C for 2 min; 30 cycles (95°C for 20 s, 56°C–64°C for 20 s, 72°C for 30 s) and 72°C for 3 min. Some amplicons had to be amplified twice to increase material density for amplicon NGS.

QUANTIFICATION AND STATISTICAL ANALYSIS

Statistical analyses and data visualization were performed using GraphPad Prism version 10. Data are shown as scatterplots, with each symbol representing an individual mouse and the horizontal line indicates the mean. Immune population frequencies in Cas9^{D10A} and C57BL/6 mice (n = 6 mice/genotype; Figure S2) were compared using two-tailed Mann–Whitney U tests, with each immune cell population analyzed independently comparing Cas9^{D10A} to C57BL/6 genotypes. Gene editing outcomes are presented as bar plots (±SD), with each symbol representing an individual mouse and the bar line indicating the mean. The frequency of each editing outcome in Cas9^{D10A} cells was compared to Cas9^{WT} cells using two-tailed Mann–Whitney U tests (n = 3–7 individual mice from 2 to 3 independent experiments). Statistical significance was defined as $p < 0.05$, and exact p-values are shown in the figures. Comparisons without an annotated p-value were performed but did not reach statistical significance. All p-values are summarized in Table S1. Information about statistical testing is additionally included in each Figure legend.